Spectrochimica Acta Part B 169 (2020) 105898

Contents lists available at ScienceDirect

Spectrochimica Acta Part B

journal homepage: www.elsevier.com/locate/sab

Characterization of the elemental composition of polish banknotes by X-ray fluorescence and laser-induced breakdown spectroscopy

Małgorzata Król[a,*], Klaudia Gondko[a], Agnieszka Kula[a], Patryk Własiuk[a], Julio M. del Hoyo-Meléndez[b], Paweł Kościelniak[a]

[a] Jagiellonian University in Kraków, Faculty of Chemistry, Department of Analytical Chemistry, 2 Gronostajowa St., 30-387 Kraków, Poland
[b] The National Museum in Krakow, Laboratory of Analysis and Non-Destructive Investigation of Heritage Objects, 14 Piłsudskiego St., 31-109 Krakow, Poland

ARTICLE INFO

Keywords:
Polish banknotes
Security features
LIBS
μXRF
Questioned document examination

ABSTRACT

In this study, two very promising techniques, micro X-ray fluorescence (μXRF) and laser-induced breakdown spectroscopy (LIBS) were applied to the examination of Polish banknotes – Polish zloty (zl).

Several areas on each banknote were selected and analysed. Different elemental compositions were identified after comparing the spectra recorded from various measurement locations. It was possible to identify characteristic atomic emissions from one or several elements such as Ca, Ti, Fe, Ba, Co, Cr, Cu, Mg, Mn, Ni, V, and Zr, depending on the banknote denomination, issue date, and evaluated spot. Potentially good discriminators with unique elemental composition were identified: black serial number (C) and microlettering (A). A comparison of brand-new banknotes with used banknotes (which have been in circulation) was also performed. The middle horizontal section of the banknotes shows higher exposure to contamination and consequently constitutes the most difficult part to analyse. Counterfeit banknotes were also analysed and were clearly distinguished from authentic notes in all cases. It was demonstrated that a comparison of the elemental composition is a useful way to detect counterfeit banknotes (10, 20, 50 and 100 zl) in 'real-world' cases.

This study shows the potential of LIBS and μXRF as effective and practical techniques to analyse Polish banknotes. Their many advantages provide a good alternative to the analytical methods routinely used for the examination of these objects.

1. Introduction

Forgery of banknotes is a major financial crime. This illegal practice, which is developing both qualitatively and quantitatively, constitutes an important problem for governments around the world. Poland is not an exception, as counterfeiting of Polish zloty (zl) banknotes is a common and current practice. The abundance of counterfeiting techniques and their continuous improvement make the task of identifying fake banknotes a very difficult one.

The characteristics of genuine banknote paper provide a form of protection against counterfeiting [1]. In Polish banknotes, a special highly resistant white fully cotton paper is employed with a weight of 80 g/m^2 and a surface refinement process that requires the use of polyvinyl alcohol. In addition, many sophisticated security features can be found including special printing techniques (micro-printing, multi-coloured notes, optically variable inks), recto-verso and latent images, watermarks, magnetic embedded strips, holograms, and luminescent areas (in UV or IR).

Although sensory inspection, based on the look, feel and tilt angle, of security features, as well as non-destructive optical and microscopic examinations [2–5] are most desirable, chemical analysis of banknotes may provide an efficient, automated and reliable methodology that enables criminal investigators to detect high-quality forgeries. Non-destructive analytical techniques have been used to examine various kinds of banknotes including, among other currencies, dollars, euros, pounds, yen, German marks, jugolire and Brazilian reals [6–20]. Micro-Raman spectroscopy and X-ray fluorescence (XRF) spectrometry have been used to analyse Hungarian postage stamps and one-lira banknotes. These two techniques have proved to be effective for determining the differences between authentic machine-produced, authentic hand-made banknotes and fake overprints, and for comparing the pigments used on authentic banknotes in circulation with those found on trial prints [9]. The coupling of atomic force microscopy (AFM) and Raman microspectroscopy was successfully applied in the discrimination of papers, pigments, and ink mixtures used in manufacturing authentic and counterfeit documents [10]. Another group of researchers [11]

* Corresponding author.
E-mail address: krolm@chemia.uj.edu.pl (M. Król).

https://doi.org/10.1016/j.sab.2020.105898
Received 23 January 2020; Received in revised form 26 May 2020; Accepted 27 May 2020
Available online 02 June 2020

demonstrated that XRF examination of major and trace elemental composition supported by multivariate statistical methods is a useful way to compare and classify counterfeit banknote papers. The potential of portable X-ray fluorescence (pXRF) spectrometry [12] and portable near-infrared spectroscopy (pNIR) [13] was shown in the examination of differently coloured regions of dollar, euro, and real banknotes. These methods were supported by chemometric methods, including principal component analysis (PCA) and partial least squares discriminant analysis (PLS-DA). Nondestructive procedures based on the analysis of several areas of euro banknotes using X-ray diffraction (XRD) [14] and micro-ATR-infrared spectroscopy [15] have been proposed to characterize and distinguish between original and counterfeit bills. A forgery detection method that uses a compact Fourier transform infrared spectrometer (FT-IR) has been developed. This method allows not only experienced scientists in laboratories, but also bank employees, police personnel, and shop workers to identify forged banknotes [16]. Mössbauer spectroscopy has been applied to the analysis of pigments in authentic and counterfeit banknotes [17]. The former contain relatively larger amounts of iron, so the detection of counterfeits is possible. The results have allowed the rapid and non-destructive identification of three types of fake banknotes: 100 USD old issue (OI) and new issue (NI) banknotes, and 50 USD NI banknotes. Desorption electrospray ionization (DESI) and easy ambient sonic-spray ionization (EASI) have been employed in the direct analysis by ambient mass spectrometry of Brazilian real, US dollar, and euro banknotes [18]. An instantaneous, reproducible, and non-destructive method for the chemical analysis of banknotes (including so-called 'real-world' counterfeits) has been developed. Electrospray laser desorption ionization mass spectrometry (LDMS), resulting in minimal damage to the banknote, was used to distinguish between authentic and counterfeit US dollars, and authentic and counterfeit new Taiwan dollars [19]. The authentic dollars had a different surface chemical composition, which was used as a marker to distinguish real banknotes from counterfeited ones. In another paper [20], LDMS was presented as an effective analytical tool for the detection and identification of security ink (e.g. Basic Red 1:1 or Basic Violet 11:1) in the presence of other colourants applied to the surface of paper (banknotes) and textiles. Although less common, there are also articles in which the destructive examination of banknotes has been reported. For instance, a rapid mass spectrometry procedure based on direct mixture analysis with conventional electron ionization was used to match pigments present on counterfeit $100 US banknotes with those contained in two suspicious inks [21]. Gas chromatography coupled to mass spectrometry (GC–MS) was used to characterize the volatile components associated with US and Canadian currencies [22].

The present study evaluates the effectiveness and usefulness of laser-induced breakdown spectroscopy (LIBS) since, to the authors' best knowledge, this technique has not been applied yet to the analysis of banknotes. A correlation of LIBS and micro X-ray fluorescence (μXRF) data – leading techniques in forensic trace elemental analysis – was also performed. The combination of these two techniques is very useful in the case of multilayer materials. The penetration depth of an X-ray beam in a sample is dependent on the elemental composition, density and absorption characteristics of that sample. Therefore, X-ray methods are often referred to as "bulk" analysis and the analyst should take precautions to minimize contamination from underneath the sample (e.g. stage or mounting media) during analysis. LIBS, on the other hand, is a surface technique. In this case, the information comes only from the ablated mass. LIBS has a small sample requirement and offers rapid, sensitive, and precise semi-quantitative elemental analysis. Compared to μXRF, LIBS is less complex to operate and has higher sample throughput (a large number of data registered in a short time). One of the main drawbacks of LIBS is its destructiveness – a small crater is visible after ablation: diameter 250–1000 μm, depth < 100 μm [23–25] depending on the physical and chemical properties of the analysed object. The second disadvantage of LIBS is the difficulty of performing an overall reliable data analysis – sometimes over 500 spectral lines need to be interpreted. During the last decade, the LIBS technique has undergone significant development [26–30]. Many different identification or classification methods [31–34], as well as quantification ones, have been applied [35–39] to support the interpretation of LIBS results. LIBS is more and more often used in various forensic examinations [40–48]. Previous literature [23–25,49–53] shows the potential of LIBS for the examination of colouring matter on paper using this technique. It was selected for the present study in order to choose the most discriminating areas on Polish banknotes based on elemental analysis. To the best of the authors' knowledge, this is the first publication that correlates results from LIBS and μXRF for forensic banknote examinations.

2. Experimental part

2.1. Instrumentation

2.1.1. μXRF

The micro-XRF analyses of the banknotes were carried out using a Bruker (Karlsruhe, Germany) Artax 800 spectrometer. This instrument is equipped with an Rh target polycapillary lens X-ray tube. The instrument has a Si drift X-ray detector, which has an active area of 10 mm^2. All spectra were collected at 50 kV and 600 mA, while the live time count used was 45 s. The measured gross count rate was around 13,000 cps and the average dead time was 3%. The analytical spot size of the instrument is approximately 0.60 mm in diameter. The beam was focused on the analysis spot with the help of a laser and a camera, which are attached to the spectrometer. X rays with high energy can completely or partially penetrate through the sample; the penetration depth is dependent on the applied energy. XRF analysis of the paper is difficult due to its minimal thickness, low density, and the low concentration of the elements of interest. The mass attenuation coefficient of paper can be approximated by assuming that the paper is 99% cellulose by mass, and that the inorganic components of the paper and inks account for about 1% of the banknote's composition. Cellulose is an organic polymer with a density of 1.5 $g{\cdot}cm^{-3}$ [54] and a mass attenuation coefficient of 0.211 $cm^{-3}{\cdot}g$ at about 50 kV [55]. The depth of penetration can be estimated using the Beer-Lambert law (Eq. (1)).

$$I = I_0 \exp(-\mu t) \quad (1)$$

where I and I_0 are the transmitted and incident photon flux, respectively; $\mu = \rho \times \sigma$ is the absorption coefficient in cm^{-1} (ρ and σ are the density and the mass absorption coefficient, respectively); and t is the thickness of the sample. On the basis of this approach, the penetration depth was estimated at 14 cm. Drake [56] and Lera et al. [57] have reported X-ray penetrations of 12.5 cm (cellulose) and 4.6 cm (paper stamps), respectively, when a tube voltage of 40 kV is employed. Penetration depth, however, can be smaller in the actual samples as not only cellulose is present on the banknotes; the chemical and physical composition of the ink can also contribute. It was observed that the radiation is capable of penetrating through the entire banknote since its thickness remains below 0.15 mm. To avoid a situation where elements in the surface of the plate below the sample are fluoresced and detected, a special sample plate was used. An empty tube of about 7 cm in height was applied so even if the radiation passed through the sample, it only encountered air space. A more accurate estimation of the penetration depth of X-rays can be carried out by preparing a series of standards containing inks with a similar composition to those found in the banknotes and using an equivalent degree of penetration of the ink into paper substrates of various thicknesses. In this way, individual lines for each element present in the inks applied on paper can be described in terms of the analytical penetration depth of the technique. However, this methodology is beyond the scope of this work and is being considered as a potential topic for future research. Acquisition and evaluation of XRF spectra were carried out using Spectra 5.3 (Bruker AXS Microanalysis, Berlin, Germany). Using this software, the net peak areas were obtained

after integral intensity calculation of the different spectral lines by Bayes deconvolution – the process of removing some signal distortions using the theoretically calculated profile as a reference.

2.1.2. LIBS

The analysis of Polish banknotes was performed using laser-induced breakdown spectroscopy system LIBS-6 (Applied Photonics, United Kingdom) with an integrated Q-switched Quantel Ultra Nd-YAG laser operating at $\lambda = 1064$ nm (Quantel, France) with a maximum energy of 150 mJ per laser pulse in 6 ns (max. Irradiance 25 GW·cm^{-2}). The diameter of the ablation spot caused by the laser was dependent on the analysed material and ranged from 0.6–1 mm. All LIBS analyses were performed under atmospheric pressure in the air. The emitted light from the LIBS plasma was collected by an Avaspec-2048-2-USB2 fibre optic Czerny-Turner spectrometer (6-channel) with a CCD detector (Avantes, The Netherlands). The emission spectrum was collected in the UV–Vis range (185–904 nm) with a spectral resolution of about 0.1 nm. The analysed object was placed on a movable table at the focal point of the focusing lens at a distance determined by the nozzle about 70 mm from the optical head. The system has a camera, giving the possibility to observe the analysed object and to aim the laser beam at the appropriate point. The LIBS-6 system was controlled by LIBSoft V6.0.1 software (Applied Photonics, United Kingdom). LIBS spectra were evaluated, and their component spectral lines were assigned using Plasus SpecLine 2.13 software (Plasus, Germany) and an NIST database (in wavelength ranges of ± 0.1 nm). During the identification process, only emission lines with intensity ≥ threefold standard deviation (SD) of signals at the noise level were taken into account.

2.2. Samples

The currency of the Polish Republic – Polish zloty (zl) – with denominations of 10, 20, 50 and 100 zl was examined. Banknotes were obtained from the National Bank of Poland (NBP) from two issues: before (old issue – OI) and after (new issue – NI) April 4th, 2014 (both brand new and used banknotes were obtained). In the analysis with μXRF, 24 samples of only brand-new polish banknotes: 12 OI (3 items per denomination), and 12 NI banknotes (3 items per denomination) were examined. In the case of LIBS examination, 52 samples were analysed: 20 brand new OI banknotes (5 items per denomination) and 20 used OI banknotes (5 items per denomination) as well as 12 brand new NI banknotes (3 items per denomination). Unfortunately, for security reasons, there is no available information on the elemental composition of printing inks used in banknotes. Prior to analysis, the banknotes were photographed, appropriately segregated and sealed in plastic bags. All banknotes were directly analysed using μXRF spectrometry and LIBS without sample pretreatment. Several areas of the banknotes on the obverse: A – F (based on denomination) and P (paper area) were analysed (see Table 1 and Fig. 1). After a careful inspection of area P on an OI banknote under the microscope (Motic, Polska), it was observed that this area had been printed on using a striped pattern (Fig. S1 (Appendix)) Thus, unfortunately, there was no place on OI banknotes where a spectrum of pure paper could be registered. Four 'real-world' counterfeit banknotes (10, 20, 50 and 100 zl from the OI) provided by the Cash and Issue Department of the National Bank of Poland were also investigated (using μXRF and LIBS) in order to compare the results obtained with those corresponding to the genuine notes.

3. Results and discussion

3.1. μXRF analysis

In order to verify the repeatability, the following examinations were performed: 1) area P of a 20 zl banknote was examined 5 times by single spot analysis in one place to estimate the influence of instrumental uncertainties (e.g. the laser shot-to-shot fluctuation); and 2) three areas (P, C, and D) of a 10 zl banknote were analysed 5 times at closely placed points (within approx. 0.25 cm^2). These three areas were selected since they have different physical features (see Table 1) and, due to that, a different chemical composition. The evaluation included a relative comparison of the raw spectra and obtained net peak areas. The results of these experiments are presented in Table 2.

In general, both matrix (e.g. absorption, secondary fluorescence) and instrumental parameter effects (e.g. background radiation, the inhomogeneous intensity distribution of the beam, sensitivity) can influence the precision of the XRF method. In our study, the precision was relatively good, the RSD values of net peak areas were lower than 10%. The lowest value was obtained for the main element that shows well-defined peaks (i.e., titanium). On the other hand, considering the repeatability of the method with 5 measurements of the same area at closely placed points, the RSD of the net peak areas oscillated around 20%. Such results showed that the peak areas strongly varied from one measurement point to another. The heterogeneity of a banknote's surface causes dissimilarities in elemental composition even for nearby measuring points. A solution to the problem of inhomogeneity could be to perform XRF elemental mapping of the entire object. X rays can go through the sample. The depth of penetration of X-rays is influenced by several factors including the density of the analysed material, the fluorescence energy of the chemical elements in the object, and the energy of the X-ray beam. In the case of banknotes – where samples are thin enough for the radiation to entirely penetrate through – elements from the other side of the banknote may be visible in the spectrum. This could be a potential source of error. Thus, it is recommended to take special precautions during the analysis of such thin objects.

Visual comparison of the 24 XRF spectra provided evidence that the elemental profiles of the examined areas were composed of: Ca, Ti, Fe, Mn, Co, Cu, Cr, and Zr in the case of OIs, whereas in current banknotes (NI) two more elements: Ni and Ba (in a very characteristic configuration) were found (see Fig. S2 and S3 (Appendix)). This confirms that the NI of banknotes is produced in a more modern way using ink with a different elemental composition. Evidently, the combination of elements detected on the various measuring areas was different (Table 3).

Furthermore, in lower denomination samples, fewer elements were detected than in 50 and 100 zl banknotes. According to these results, it could be ascertained that OI 10 and 20 zl Polish banknotes have the least varied elemental content. Probably due to their relatively lower value, they seem to be less protected in terms of security features [58]. Independently of the banknote denomination, the ratios of the main elements (net areas) showed interesting relations. In the case of OIs, three examined areas showed a unique elemental composition: 1) area A with Ti and Ca contents on a high level: [Ti] ≅ [Ca], 2) area C with Fe and Ti elements: [Ti] ≅ 1/3[Fe], and 3) area E (found only on 50 and 100 zl banknotes) with a significant content of Ti and Cr: [Ti] ≅ 4 [Cr].

After evaluating the spectra of NIs, two measuring areas attracted attention: 1) area A with high levels of Ti and Ca: [Ti] ≅ [Ca], and an additional element namely, Ba, in 50 and 100 zl banknotes, 2) area E (only on 50 and 100 zl notes) with content of Ti, Cr and Ni: [Ti] ≅ 1/3[Cr] ≅ 4[Ni].

Thus, these results along with a visual comparison indicated that these areas were the best options for verifying the authenticity of banknotes.

3.2. Statistical analysis of XRF results

The analysis of μXRF data was carried out on three datasets, each described by three independent variables. Banknotes of all analysed denominations all together; 10 and 20 zl; and 50 and 100 zl were treated as separate datasets (γ, α, and β, respectively). Dependent variables, namely net areas of Ca, Ti and Fe normalized to Rh net area, were chosen because of their presence in all analysed samples. Three independent variables were considered: measurement area, issue, and denomination.

Table 1
Analysed areas of Polish banknotes.

Measuring area	Object	Location	Colour	Ink
A	microlettering (repeated letters RP)	within a separate field in the background of a number on the top right-hand side	colouring of the entire banknote: brown-greenish (10 zl), pinkish (20 zl), blueish (50 zl), greenish (100 zl)	nd
B	serial number (two capital letters and seven digits)	printed horizontally (10 and 20 zl) or vertically (50 and 100 zl) on the front of note on the lower right-hand side	red (orange in UV)	nd
C	serial number (two capital letters and seven digits)	printed horizontally on the front of note on the lower left-hand side	black	nd
D (only on 10 zl and 20 zl)	Romanesque rosettes (10 zl) bricks crowning Romanesque portal and minor details within the portal (20 zl)	in the middle of note next to the ruler's portrait	grey (willow-green in UV light)	metallised ink
E (only on 50 zl and 100 zl)	crowned letter K (50 zl), rosette (100 zl)	on the front of the note, on the right of portrait	changes colour from pink to grey-green (OI), from blue to green (NI, 50 zl) or from gold to green (NI, 100 zl) depending on the angle of vision	optically variable ink
F (only on 100 zl)	metallic overcoating	on the front of the note, within rosette on the left of the portrait	gold	nd
P	paper with the composition of guilloche line (OI) or pure paper (NI)	the left-hand side of the note	colouring of the entire banknote (OI) or white (NI)	nd

OI – old issue, NI – new issue, nd – no data.

Since the assumptions for the ANOVA were not met, non-parametric Kruskal-Wallis one-way analysis of variance by ranks was employed. This test is aimed at comparing samples from k groups of independent observations ($k > 2$) with the null hypothesis stating that the groups are sampled from populations with identical distributions with the alternative that at least two are sampled from different populations. It is based on the H statistic, calculated using sums for ranked data, and approximated by a chi-square distribution with k-1 degrees of freedom ($\chi^2(k-1)$) at $\alpha = 0.05$. The statistical decision is to reject the null hypothesis when $H > \chi^2(k-1)$, suggesting that the data provide sufficient evidence to conclude that there are significant differences among the groups.

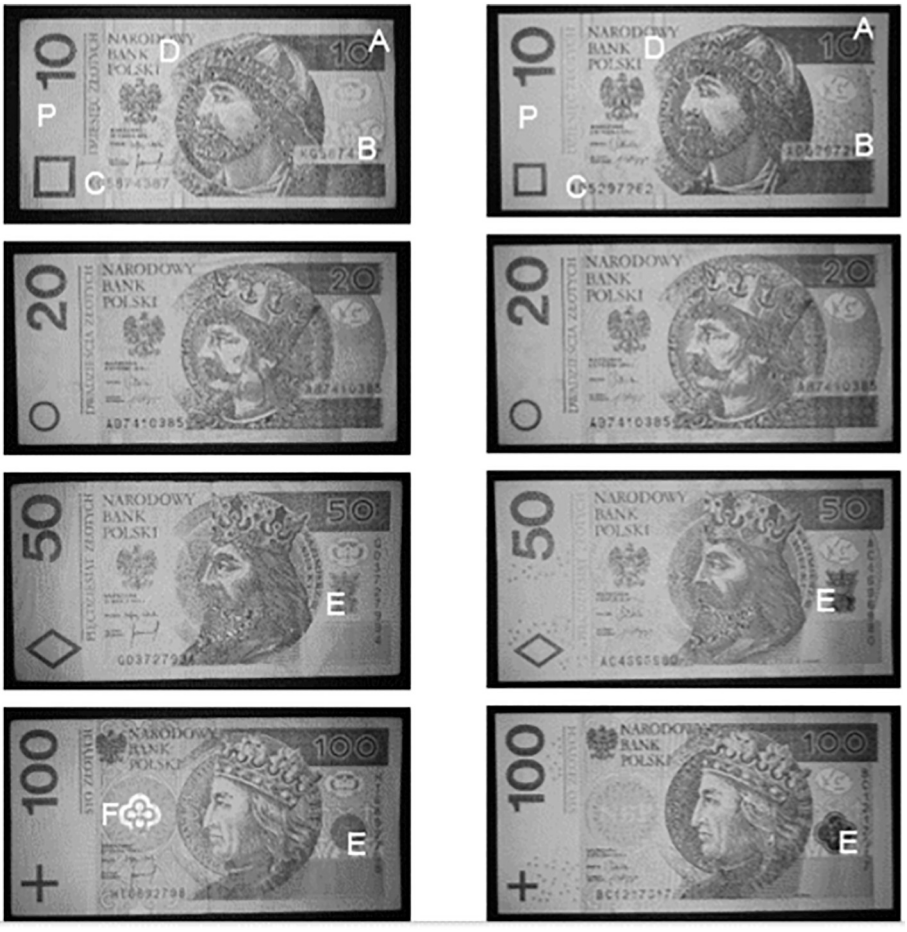

Fig. 1. Analysed areas on Polish banknotes: OI, before April 2014 (left column); NI, after April 2014 (right column).

Table 2
Repeatability of net peak areas (NPA) obtained for the analysed banknotes using μXRF.

Sample	Description of acquisition procedure	Parameter	Element/energy (keV)						
			K /3.314	Ca /3.692	Ti /4.512	Fe /6.405	Mn /5.900	Co /6.931	Cu /8.046
20 zl point P	5 measurements by single spot analysis in one place	Average NPA	4301	4960	110,058	3118	–	–	–
		RSD (%)	1.0	9.4	0.6	7.9	–	–	–
10 zl point P	5 measurements of the same area (in closely placed points)	Average NPA	2570	3380	184,592	6027	–	–	–
		RSD (%)	14	5.6	12	33	–	–	–
10 zl point C	5 measurements of the same area (in closely placed points)	Average NPA	1853	47,773	154,566	493,989	9737	24,361	12,502
		RSD (%)	33	23	22	15	15	15	33
10 zl point D	5 measurements of the same area (in closely placed points)	Average NPA	1251	3181	125,784	4056	–	–	–
		RSD (%)	38	24	8.9	13	–	–	–

Table 3
Elemental profiles obtained by XRF analysis for various areas of Polish banknotes of all denominations.

Sample area	Ca	Fe	Ti	Ba	Co	Cr	Cu	Mn	Ni	Zr
old issue (OI)										
A	+	+	+	−	+	−	+	+	−	+
B	+	+	+	−	+	−	+	+	−	−
C	+	+	+	−	+	−	+	+	−	−
D (10 and 20)	+	+	+	−	−	−	−	−	−	−
E (50 and 100)	+	+	+	−	+	+	−	+	−	+
new issue (NI)										
A	+	+	+	+[a]	+[b]	−	+	+	−	+
B	+	+	+	−	+	−	+	+	−	−
C	+	+	+	+[c]	+	−	+[a]	+	−	−
D (10 and 20)	+	+	+	−	−	−	−	−	−	−
E (50 and 100)	+	+	+	−	−	+	−	−	+	−

[a] only for 50 and 100 zl, [b] only for 10 and 20 zl, [c] only for 100 zl.

It was established, that statistically significant ($p < .01$) differences in all datasets were recognized when analysing Ca and Fe composition and different measurement areas: $\chi^2(4) = 36.4$, $\chi^2(4) = 27.2$, $\chi^2(3) = 57.3$ for Ca in β, α and γ dataset, respectively, and for Fe: $\chi^2(4) = 15.4$, $\chi^2(4) = 22.1$, $\chi^2(3) = 24.0$. This provides evidence to suggest that there is a difference between at least one pair of measurement areas. The Ti variable recognizes the difference among groups related to the issue ($\chi^2(1) = 25.0$, $\chi^2(1) = 10.4$, $\chi^2(1) = 28.7$ in β, α and γ datasets, respectively, ($p < .01$). However, this information is of limited use since visual inspection of banknotes provides an immediate answer.

In order to indicate a specific measurement area that differs significantly, a Nemenyi post-hoc test for pairwise multiple comparisons of the ranked data was applied to each of the datasets based on Ca and Fe content separately. The results are presented in Fig. 2. Areas A and C might be considered potential discriminatory points for banknotes regardless of their denomination or issue designation. The distinction between different datasets comprised of 10 and 20 zl banknotes as well as 50 and 100 zl banknotes seems to indicate that area D might be disregarded from the former dataset (10 and 20 zl) and the inclusion of measurement area E in the latter dataset is worth considering. Nevertheless, the dataset based on all banknotes confirms the results from visual interpretation (see section 3.1.).

3.3. LIBS optimization

In order to obtain reliable and most informative emission spectra of banknotes, an optimization procedure of the LIBS method was conducted. The main criterion for the selection of optimal analysis parameters was to obtain the largest possible number of signals and relatively high signal intensity (the discriminatory elements mainly occurred in trace amounts) without saturation of the spectrum. The amount of sample consumed and the size of resultant craters were also taken into consideration, in order to reduce the amount of ablated paper.

In the first step, the Q-switch delay [μs] was optimized. It is inversely proportional to the laser power. Maximum power = 25 MW is equal to Q-switch delay = 135 μs. For this purpose, a new 10 zl banknote was used and a series of measurements were carried out in the range of Q-switch delay from 135 to 255 μs. The optimal value was found to be 135 μs requiring the maximum power of the laser.

The next optimization step focused on the detector parameters, including gate delay (1.27–1.35 μs) and integration time (1.1–1.4 ms). In the case of gate delay, increasing the time resulted in decreasing signal intensities. Therefore, all measurements were performed with a gate delay of 1.27 μs. Regarding the integration time, the best spectra were obtained when their recording lasted 1.4 ms.

It was found that the conditioning shot, used for cleaning contamination from the surface before analysis, not only did not improve the spectrum but also caused spectral distortion. In fact, it was observed that the layer of colouring matter on the surface of the paper was so thin that a single laser shot was sufficient to penetrate through it and also cause ablation of the paper. Thus, a single accumulation was found optimal both for reducing sample destruction (Fig. S4 (Appendix)) and for obtaining an adequate and reliable spectrum. However, it was observed that a spectrum based on five shots yielded a significant enhancement of the S/N ratio. Therefore, data were collected from 5 different points of the same measuring area.

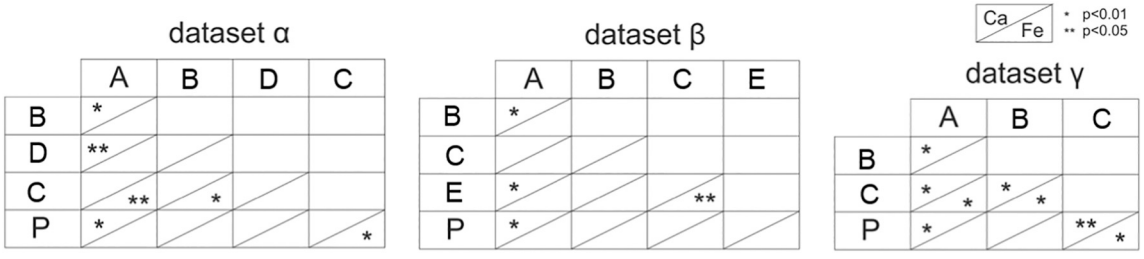

Fig. 2. Matrices of pairwise comparisons (statistical significance reported as *p*-values) using the Nemenyi test with chi-squared approximation for independent samples of three datasets (α = 10 and 20 zl banknotes, β = 50 and 100 zl banknotes, γ = all banknotes).

Table 4
The repeatability of peak intensities (the most intense ones) of elements obtained for the analysed banknotes using LIBS.

Sample	Description of the acquisition procedure	Para-meter	Ca	Ti	Fe	Mn	Co	Cu	Cr
10 zl (NI) area P	5 measurements of the same area (moving the object)	Int. (V)	8374	24,608	–	–	–	–	4045
		λ (nm)	*501.9*	*501.4*					*429.0*
		RSD (%)	15	11	–	–	–	–	16
10 zl (OI)		Int. (V)	13,416	31,147	–	–	–	–	6015
area P		λ (nm)	*501.9*	*501.4*					*429.0*
		RSD (%)	24	20	–	–	–	–	25
10 zl area C		Int. (V)	1547	11,439	23,869	2580	5088	8935	–
		λ (nm)	*442.5*	*499.1*	*438.3*	*403.3*	*352.6*	*510.6*	
		RSD (%)	23	29	29	28	29	21	–
10 zl area D		Int. (V)	11,909	–	1976	4460	2439	–	–
		λ (nm)	*443.5*		*382.0*	*403.3*	*357.0*		
		RSD (%)	27	–	34	33	42	–	–

In order to evaluate the repeatability of the results, analyses of different measuring areas (5 repetitions) were performed on new 10 zl banknotes, both from OI and NI. The positions (wavelengths) of the spectral lines detected for the analysed samples were repeatable. Successive spectra only differed in the intensities of the signals (see Table 4), which are mainly related to the laser shot-to-shot fluctuation, the unrepeatable phenomenon of plasma creation and cooling, and the chosen place of analysis (the heterogeneity of the sample composition). The intensities of the most intense persistent lines for several elements varied from one measuring area to another, with an RSD value that ranged from 11.1 to 41.6. The lowest RSD was obtained for pure paper (10 zl NI), while the highest corresponded to metallic printing ink. Thus, to improve repeatability, the average spectrum obtained from five measurements in one measuring area was recorded after gently moving (within an area of 0.25 cm^2) the banknote, which was placed on a sample plate.

3.4. LIBS analysis

LIBS spectra from measuring area P for: 1) 5 brand new OI banknotes, 2) 5 used OI banknotes, and 3) 3 brand new NI banknotes were recorded under the optimized experimental conditions. Spectra registered for banknote papers were quite different from the spectrum of standard office paper [59]. The banknote paper gave a richer spectrum with a higher number of lines originating from neutral species (I), singly charged ions (II), and molecules (see Fig. 3). The presence of several elements such as Ti, Ca, Na, K, Al, and Cr was revealed. The presence of Ti was most likely related to the use of titanium dioxide during the beating process of cotton paper pulps in order to improve the fibrillation of cotton fibres and the distribution of fillers. The elemental characteristics of banknote paper might be used as a first step in the identification of fake banknotes.

Only quantitative differences in the elemental composition of paper were observed after comparing brand new banknotes from the same issue. On the other hand, there were dissimilarities between banknote papers from NI and OI. This was probably a consequence of the striped pattern of printing ink found in OI banknotes. Only the spectrum of NI banknotes (Fig. 4, red line) can be assumed to be derived solely from the emission spectrum of blank paper. In this study, the banknote was treated as an integrated system consisting of paper and colouring matter produced with high production standards, and accordingly, it was analysed as an inseparable sample.

To verify how impurities influence results, brand new banknotes were compared with used ones. For this purpose, averaged spectra corresponding to the same elemental measurement areas on new and used banknotes (of various denominations) were superimposed and studied signal by signal. In general, the results allowed the banknotes to be separated into two groups. The first group contained banknotes that do not differ from each other qualitatively, while in the second group the spectra of the used banknote contained additional spectral lines. For instance, after careful observation of the spectrum of a 10 zl banknote, several additional emission lines were visible (Fig. 4). These were persistent lines originating from Fe I: 371.965, 373.457, 373.670, 374.572, 374.942). The possible reason for the appearance of new spectral lines is the fact that these banknotes were used by people and show signs of contamination derived from many different sources, including hands, metal parts of wallets, purses, or pockets. The places showing higher exposure to contaminants are measuring areas B, C, and P, independently of the denomination, D on 10 and 20 zl bills, and F on 100 zl banknotes. On the other hand, the same emission spectra for the

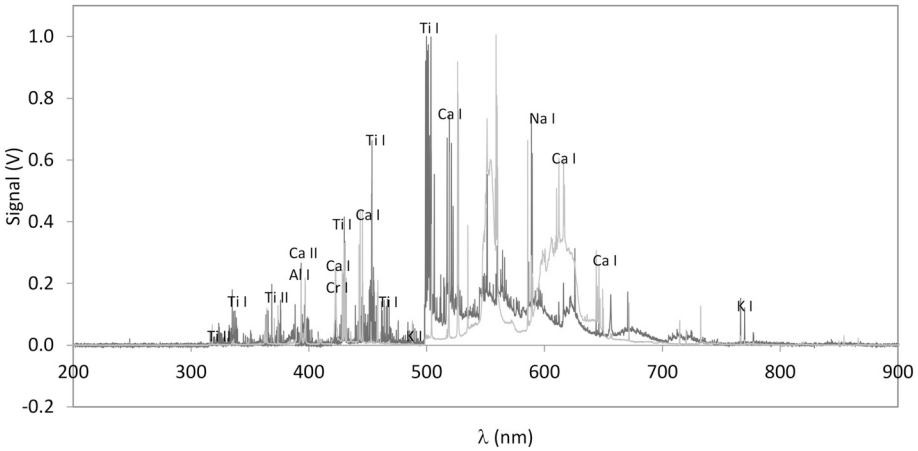

Fig. 3. LIBS spectrum registered on area P of a 10 zl banknote (blue) compared with the spectrum of standard office paper (red). (For interpretation of the references to colour in this figure legend, the reader is referred to the web version of this article.)

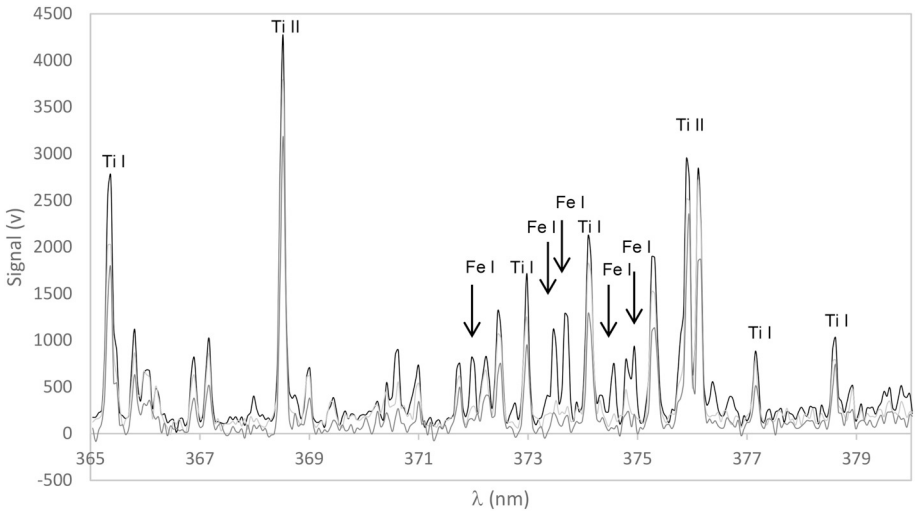

Fig. 4. Fragment of LIBS spectra of three 10 zl banknotes registered in area P: brand new OI banknote (green), used OI banknote (blue), brand new NI banknote (red). Peaks originating from impurities are indicated by arrows. (For interpretation of the references to colour in this figure legend, the reader is referred to the web version of this article.)

new and used banknotes were obtained in the case of area A on 10 and 20 zl notes, and areas A and E on 50 and 100 zl bills. A possible explanation for these relationships is based on their continuous use. For example, when taking a Polish banknote from a wallet, a person frequently grasps it in the middle (lengthwise), covering the portrait with a finger. However, when a Polish banknote is handed over to another person, usually the giver grasps it around the red serial number whilst the recipient takes the banknote from the opposite side. It is very important to take contamination into account when carrying out analysis of used banknotes. It must always be determined whether the differences are caused by counterfeiting or contamination. Analyses can be performed after attempts to gently clean the surface of the banknote. In doubtful situations, it is recommended to compare the elemental profile in other measuring areas with high discriminatory potential and with less likelihood of contamination.

The elemental composition obtained from LIBS for selected measuring areas is listed in Table 5. The results differed from those originating from μXRF analysis but also showed technological dissimilarities in OI and NI banknotes manifesting in different elemental compositions of the same measuring areas (e.g. Ba in area A). On the other hand, the most common element found in almost every measuring area independently of issue is Mn. In some cases, XRF detected a larger number of elements in a particular measuring area, e.g. area A or B (compare Tables 3 and 5). However, there were also areas, for instance, C, D, and E, where a richer elemental composition was found by the LIBS technique. It is very difficult to find a clear correlation here. The different penetration depth and sensitivity of the two techniques were probably the reasons for these variations. It is worth mentioning that in the case of LIBS, the criteria applied during the interpretation of spectral lines were crucial [60,61]. For instance, Ni yielded a large number of low-intensity signals (almost at the noise level), which cannot be interpreted as significant spectral lines. What is more, there were cases in which many intense lines came from one element (e.g. Fe), but none of them was labelled as persistent in the NIST database. Under the established interpretation criteria, there were no grounds to claim that it was present. Furthermore, in contrast to XRF, LIBS elemental profiles from OI banknotes were relatively richer than those from their NI counterparts. A selection of the most discriminating areas was possible taking into account such qualitative information. In the case of OIs, the most unique elemental profile was in area C, whereas in the case of NIs there were three characteristic areas: 1) A for Ba, 2) C for Co, and 3) E for Mg.

Table 5
Elemental profiles obtained by LIBS analysis for various areas of Polish banknotes of all denominations.

LIBS	Ca	Fe	Ti	Ba	Co	Cr	Cu	Mn	Ni	Zr	Mg	V
old emission (OI)												
A	+	−	+	−	−	−	−	+[a]	−	+	−	−
B	+	+	+	−	−	−	−	+	−	+[b]	−	−
C	+	+	+	−	+	+	+[c]	+	+	+	+	+
D (10 and 20)	+	+	+	−	+	+	+[d]	+	−	+	+	+
E (50 and 100)	+	−	+	−	−	+	−	+	−	+	+	−
new emission (NI)												
A	+	−	+	+[b]	−	−	−	+[e]	−	+	−	−
B	+	−	+	−	−	−	−	+	−	−	−	−
C	+	−	+	−	+[f]	−	−	+	−	+	−	−
D (10 and 20)	+	−	+	−	−	−	−	−	−	−	−	−
E (50 and 100)	+	−	+	−	−	−	−	−	−	−	+	−

[a] apart from 100 zl, [b] only for 50 and 100 zl, [c] apart from 10 zl, [d] only for 20 zl, [e] only for 10 zl, [f] only for 100 zl.

3.5. Statistical analysis of LIBS results

Similarly to the data obtained from XRF, three datasets described by three independent variables were investigated: γ – banknotes of all denomination, α: 10 and 20 zl, and β: 50 and 100 zl banknotes. The intensities of spectral lines (persistent ones) of three elements (Ti, Ca and Zr) present in all analysed banknotes (only in areas A and C) were selected as dependent variables. Independent variables were the same as in the case of XRF data namely– measurement area, issue, and denomination.

Due to the inhomogeneity of variances, a non-parametric method – Kruskal-Wallis one-way analysis of variance by ranks – was performed, as was done in the case of XRF data analysis. When the measuring area was considered as an independent variable, statistically significant ($p < .01$) differences were recognized in Zr compositions between different areas in the γ dataset ($\chi^2(1) = 32.1$), in Ca composition for the α dataset ($\chi^2(1) = 16.1$), and in Ti composition for the β dataset ($\chi^2(1) = 9.0$). There were no statistically significant differences among groups organized by denomination. Taking into account the different issues (OI and NI), the Zr composition revealed statistically significant differences ($\chi^2(1) = 10.8$, $\chi^2(1) = 21.1$, $\chi^2(1) = 6.58$ for α, β, and γ datasets, respectively, ($p < .01$).

A post-hoc test was not performed since only two areas (A and C) were analysed. These two areas can be considered potential discriminatory points for Polish banknotes, which is in accordance with the visual assessments.

3.6. Case studies results

After the analysis of the collected original banknotes, μXRF and LIBS analyses of suspected counterfeits were conducted using the same

methodology. The four different specimens of 10, 20, 50 and 100 Polish zloty banknotes from OI suspected to be counterfeited were investigated. All measurements were performed on area C – the black serial number – which was previously statistically selected as one of the most discriminatory parts of the banknote. In all four cases, it was possible to discriminate between counterfeit and authentic banknotes. The comparison criterion was based on the qualitative presence/absence of elements and semi-quantitative data. The variation of elemental profiles within area C of individual counterfeits and between areas C of the four counterfeits was smaller than the variation for genuine banknotes. A comparison of the obtained results revealed that every suspected banknote was made with the use of standard office paper, not banknote paper. Both the element profiles and the ratios of detected elements of the 4 examined samples were different from those of genuine banknotes. For instance, in the case of μXRF results, unique characteristics for area C elemental composition ([Ti] ≅ [1/3[Fe]) was not observed. Considering the LIBS results for area C, additional spectral lines from aluminium appear for the 100 and 50 zl banknotes, but there are no lines characteristic for Co, Cr, and Ni. Thus, on the basis of the obtained results, the proposed procedure could be applied to the detection of fakes of any denomination.

4. Conclusions

The effectiveness of LIBS in the analysis of Polish banknotes was assessed and compared with that of μXRF. Although both techniques gave reproducible and comparable results, particular caution is advisable when evaluating the data. In LIBS, problematic spectral noise manifested by the presence or absence of different emission lines may be observed. The noise was dependent on the characteristic plasma evolution, which is a consequence of the laser fluctuation as well as the detector gate delay selected. This complicated the elemental interpretation. However, once this problem was solved by careful selection of valid spectral lines, reproducible spectra concerning qualitative differences between the same areas of banknotes were obtained. It was found that there was a consistent composition of the ink and the paper between different banknotes of the same denomination and issue, respectively.

This confirms the use of high-quality control standards in the production of banknotes starting from the paper and ending with a variety of security features. However, the radiation employed in μXRF has the ability to penetrate entirely through the sample resulting in misinformation, since elements from the second side of the banknote may be detected in the spectrum.

Considering the quantitative repeatability of the LIBS method, RSD values oscillated around 28%. After comparing it with μXRF, it was found that the RSD of the net peak areas was lower (about 20%). However, in both cases, the intensities/areas of the lines strongly varied from one measuring point to another. A possible way of overcoming the inhomogeneity problem is to work with both techniques in elemental imaging (mapping) mode. Scanning a sample beneath the X-ray microbeam or the laser beam allows detailed hyperspectral elemental images to be obtained. These contain both spatial and spectral information which can be used to study element distribution.

The results also indicate that LIBS allows us to distinguish individual features of a banknote. Identification of the obtained lines provided enough evidence about specific elemental profiles for each particular measurement area. However, LIBS elemental compositions were different from those detected using μXRF. This is a complex issue, presumably related to the physicochemical principles (e.g. penetration of radiation) and sensitivity of each technique. The protocols employed during the interpretation of LIBS spectral lines – at least two persistent lines of an element were required to give grounds to claim that it was present – were also very important. The sensitivity of LIBS is theoretically greater. Due to the lack of adequate standards, it was very difficult to estimate the actual difference. Regarding the interpretation criteria, there were cases in which a lot of intense lines coming from one particular element were observed in the LIBS spectrum, but none of them was persistent. Such signals should not be unequivocally interpreted as significant spectral lines.

Nevertheless, thanks to a very careful analysis of the LIBS emission spectra, many differences between the measuring areas were observed. The most characteristic spectrum was obtained for the points C, A, and E (on 50 and 100 zl banknotes, especially in the case of NI). This is consistent with μXRF results and was confirmed by statistical analysis. In conclusion, the developed LIBS method can be used for the analysis of banknotes since the results can be relevant for judicial purposes. However, the number of banknotes used in the study was relatively small and therefore larger datasets are needed to report the power of the test, to estimate error rates and uncertainty, and to be able to generalize the above-mentioned conclusions. Given its low cost, high sample throughput, and ease of use, the application of LIBS to banknote examination has been shown to be as effective as μXRF. In summary, LIBS is a viable alternative to μXRF, but a multi-method approach provides an adequate more effective and reliable way of comparing and validating the results.

Future research includes analysing a larger number of used banknotes in order to better assess the most frequently found impurities. This will allow us to evaluate the adequacy of the proposed methods for routine forensic analysis. It is worth emphasizing at this point that additional studies involving more ‘real-world’ counterfeit banknotes should also be performed.

Acknowledgements

This work was supported by the Ministry of Science and Higher Education, Poland for their financial support (grant no. IP2012025672) and the European Regional Development Fund, European-Union within the framework of the Polish Innovation Economy Operational Program (contract no. POIG.02.01.00-12-023/08). The authors gratefully acknowledge Narodowy Bank Polski for providing the authentic and counterfeit banknotes used for this study.

Declaration of Competing Interest

The authors declare that they have no known competing financial interests or personal relationships that could have appeared to influence the work reported in this paper.

Appendix A. Supplementary data

Supplementary data to this article can be found online at https://doi.org/10.1016/j.sab.2020.105898.

References

[1] https://www.pwpw.pl/en/Products/Banknotes/Banknotes.html (accessed 13 Jan. 2020).
[2] A. Bruna, G.M. Farinella, G.C. Guarnera, S. Battiato, Forgery detection and value identification of euro banknotes, Sensors 13 (2013) 2515–2529, https://doi.org/10.3390/s130202515.
[3] T.H. Chia, M.J. Levene, Detection of counterfeit U.S. paper money using intrinsic fluorescence lifetime, Opt. Express 17 (2009) 22054–22061, https://doi.org/10.1364/OE.17.022054.
[4] J. Takalo, J. Timonen, J. Sampo, M. Rantala, S. Siltanen, M. Lassas, Using the fibre structure of paper to determine authenticity of the documents: analysis of transmitted light images of stamps and banknotes, Forensic Sci. Int. 244 (2014) 252–258, https://doi.org/10.1016/j.forsciint.2014.09.002.
[5] H.-T. Lim, V.M. Murukeshan, Hyperspectral imaging of polymer banknotes for building and analysis of spectral library, Opt. Lasers Eng. 98 (2017) 168–175, https://doi.org/10.1016/j.optlaseng.2017.06.022.
[6] A. Guedes, M. Algarra, A.C. Prieto, B. Valentim, V. Hortelano, S. Neto, R. Algarra, F. Noronha, Raman microspectroscopy of genuine and fake euro banknotes, Spectrosc. Lett. 46 (2013) 569–576, https://doi.org/10.1080/00387010.2013.769007.
[7] M. Skenderović Božičević, A. Gajović, I. Zjakić, Identifying a common origin of

toner printed counterfeit banknotes by micro-Raman spectroscopy, Forensic Sci. Int. 223 (2012) 314–320, https://doi.org/10.1016/j.forsciint.2012.10.007.
[8] M.R. de Almeida, D.N. Correa, W.F.C. Rocha, F.J.O. Scafi, R.J. Poppi, Discrimination between authentic and counterfeit banknotes using Raman spectroscopy and PLS-DA with uncertainty estimation, Microchem. J. 109 (2013) 170–177, https://doi.org/10.1016/j.microc.2012.03.006.
[9] I.J. Badovinac, N. Orlić, C. Lofrumento, J. Dobrinić, M. Orlić, Spectral analysis of postage stamps and banknotes from the region of Rijeka in Croatia, Nucl. Instrum. Meth. A 619 (2010) 487–490, https://doi.org/10.1016/j.nima.2009.10.174.
[10] J.M.O.B. Brandão, N.S.M. Almeida, P.V.M. Dixini, C.H.A. Baier, H.P. Dias, J.F.P. Bassane, H.S. França, S.R.C. Silva, G.M.F.V. Aquije, W. Romão, Documentoscopy by atomic force microscopy (AFM) coupled with Raman microspectroscopy: applications in banknote and driver license analyses, Anal. Methods-UK 8 (2016) 771–784, https://doi.org/10.1039/C5AY03128A.
[11] H. Guo, B. Yin, J. Zhang, Y. Quan, G. Shi, Forensic classification of counterfeit banknote paper by X-ray fluorescence and multivariate statistical methods, Forensic Sci. Int. 266 (2016) e43–e47, https://doi.org/10.1016/j.forsciint.2016.06.008.
[12] C.R. Appoloni, F.I. Melquiades, Portable XRF and principal component analysis for bill characterization in forensic science, Appl. Radiat. Isot. 85 (2014) 92–95, https://doi.org/10.1016/j.apradiso.2013.12.004.
[13] R.M. Correia, E. Domingos, F. Tosato, L.F.M. Aquino, A.M. Fontes, V.M. Cáo, P.R. Filgueiras, W. Romão, Banknote analysis by portable near infrared spectroscopy, Forensic Chem. 8 (2018) 57–63, https://doi.org/10.1016/j.forc.2018.02.003.
[14] D. Marabello, P. Benzi, A. Lombardozzi, M. Strano, X-ray powder diffraction for characterization of raw materials in banknotes, J. Forensic Sci. 62 (2017) 962–970, https://doi.org/10.1111/1556-4029.13392.
[15] A. Vila, N. Ferrer, J. Mantecón, D. Bretón, J.F. García, Development of a fast and non-destructive procedure for characterizing and distinguishing original and fake euro notes, Anal. Chim. Acta 559 (2006) 257–263, https://doi.org/10.1016/j.aca.2005.11.084.
[16] E. Sonnex, M.J. Almond, J.V. Baum, J.W. Bond, Identification of forged Bank of England £20 banknotes using IR spectroscopy, Spectrochim. Acta A-M 118 (2014) 1158–1163, https://doi.org/10.1016/j.saa.2013.09.115.
[17] V. Rusanov, K. Chakarova, H. Winkler, A.X. Trautwein, Mössbauer and X-ray fluorescence measurements of authentic and counterfeited banknote pigments, Dyes Pigments 81 (2009) 254–258, https://doi.org/10.1016/j.dyepig.2008.07.020.
[18] L.S. Eberlin, R. Haddad, R.C. Sarabia Neto, R.G. Cosso, D.R.J. Maia, A.O. Maldaner, J. Jardim Zacca, G.B. Sanvido, W. Romão, B.G. Vaz, D.R. Ifa, A. Dill, R.G. Cooks, M.N. Eberlin, Instantaneous chemical profiles of banknotes by ambient mass spectrometry, Analyst 135 (2010) 2533–2539, https://doi.org/10.1039/c0an00243g.
[19] Y. Kao, Ch. Cheng, S. Cheng, H. Ho, J. Shiea, Distinguishing authentic and counterfeit banknotes by surface chemical composition determined using electrospray laser desorption ionization mass spectrometry, J. Mass Spectrom. 48 (2013) 1129–1135, https://doi.org/10.1002/jms.3263.
[20] L. Balko, J. Allison, The direct detection and identification of staining dyes from security inks in the presence of other colorants, on currency and fabrics, by laser desorption mass spectrometry, J. Forensic Sci. 48 (2003) 1172–1178, https://doi.org/10.1520/jfs2003062.
[21] A. Acampora, P. Ferranti, A. Malorni, A. Milone, Mass spectrometry in forensic chemistry: 1. Pigment identification by direct mixture analysis in a case of bank note falsification, J. Forensic Sci. 36 (1991) 579–586, https://doi.org/10.1520/JFS13062J.
[22] D.T. Vu, Characterization and aging study of currency ink and currency canine training aids using headspace SPME/GC-MS, J. Forensic Sci. 48 (2003) 754–770 10.1520/JFS2002280.
[23] A. Kula, R. Wietecha-Posłuszny, K. Pasionek, M. Król, M. Woźniakiewicz, P. Kościelniak, Application of laser induced breakdown spectroscopy to examination of writing inks for forensic purposes, Sci. Justice 54 (2014) 118–125, https://doi.org/10.1016/j.scijus.2013.09.008.
[24] T. Trejos, A. Flores, J.R. Almirall, Micro-spectrochemical analysis of document paper and gel inks by laser ablation inductively coupled plasma mass spectrometry and laser induced breakdown spectroscopy, Spectrochim. Acta B 65 (2010) 884–895, https://doi.org/10.1016/j.sab.2010.08.004.
[25] A. Metzinger, R. Rajkó, G. Galbács, Discrimination of paper and print types based on their laser induced breakdown spectra, Spectrochim. Acta B 94-95 (2014) 48–57, https://doi.org/10.1016/j.sab.2014.03.006.
[26] M.Z. Martin, N. Labbé, N. André, R. Harris, M. Ebinger, S.D. Wullschleger, A.A. Vass, High resolution applications of laser-induced breakdown spectroscopy for environmental and forensic applications, Spectrochim. Acta B 62 (2007) 1426–1432, https://doi.org/10.1016/j.sab.2007.10.046.
[27] D.W. Hahn, N. Omenetto, Laser-induced breakdown spectroscopy (LIBS), part II: review of instrumental and methodological approaches to material analysis and applications to different fields, Appl. Spec. 66 (2012) 347–419, https://doi.org/10.1366/11-06574.
[28] G. Galbács, A critical review of recent progress in analytical laser-induced breakdown spectroscopy, Anal. Bioanal. Chem. 407 (2015) 7537–7562, https://doi.org/10.1007/s00216-015-8855-3.
[29] R. Noll, C. Fricke-Begemann, S. Connemann, Ch. Meinhardt, V. Sturm, LIBS analyses for industrial applications – an overview of developments from 2014 to 2018, J. Anal. At. Spectrom. 33 (2018) 945–956, https://doi.org/10.1039/c8ja00076j.
[30] L. Jolivet, M. Leprince, S. Moncayo, L. Sorbier, C.-P. Lienemann, V. Motto-Ros, Review of the recent advances and applications of LIBS-based imaging, Spectrochim. Acta B 151 (2019) 41–53, https://doi.org/10.1016/j.sab.2018.11.008.
[31] G. Amato, G. Cristoforetti, S. Legnaioli, G. Lorenzetti, V. Palleschi, F. Sorrentino, E. Tognoni, Progress towards an unassisted element identification from laser induced breakdown spectra with automatic ranking techniques inspired by text retrieval, Spectrochim. Acta B 65 (2010) 664–670, https://doi.org/10.1016/j.sab.2010.04.019.
[32] T.F. Boucher, M.V. Ozanne, M.L. Carmosino, M.D. Dyar, S. Mahadevan, E.A. Breves, K.H. Lepore, S.M. Clegg, A study of machine learning regression methods for major elemental analysis of rocks using laser-induced breakdown spectroscopy, Spectrochim. Acta B 107 (2015) 1–10, https://doi.org/10.1016/j.sab.2015.02.003.
[33] P. Pořízkaa, J. Klusa, E. Képeš, D. Prochazka, D.W. Hahn, J. Kaiser, On the utilization of principal component analysis in laser-induced breakdown spectroscopy data analysis, a review, Spectrochim. Acta B 148 (2018) 65–82, https://doi.org/10.1016/j.sab.2018.05.030.
[34] D. Syvilay, J. Guezenoc, B. Bousquet, Guideline for increasing the analysis quality in laser-induced breakdown spectroscopy, Spectrochim. Acta B 161 (2019) 105696, , https://doi.org/10.1016/j.sab.2019.105696.
[35] J.-B. Sirven, B. Bousquet, L. Canioni, L. Sarger, Laser-induced breakdown spectroscopy of composite samples: comparison of advanced chemometrics methods, Anal. Chem. 78 (2006) 1462–1469, https://doi.org/10.1021/ac051721p.
[36] J. Yang, C. Yi, J. Xu, X. Ma, Laser-induced breakdown spectroscopy quantitative analysismethod via adaptive analytical line selection and relevance vector machine regression model, Spectrochim. Acta B 107 (2015) 45–55, https://doi.org/10.1016/j.sab.2015.02.014.
[37] T. Takahashi, B. Thornton, Quantitative methods for compensation of matrix effects and self-absorption in laser induced breakdown spectroscopy signals of solids, Spectrochim. Acta B 138 (2017) 31–42, https://doi.org/10.1016/j.sab.2017.09.010.
[38] Shan Wu, Tianlong Zhang, Hongsheng Tang, Kang Wang, Xiaofeng Yang, Hua Li, Quantitative analysis of nonmetal elements in steel using laser-induced breakdown spectroscopy combined with random forest, Anal. Methods 7 (2015) 2425–2432, https://doi.org/10.1039/c4ay02601b.
[39] J. Guezenoc, A. Gallet-Budynek, B. Bousquet, Critical review and advices on spectral-based normalization methods for LIBS quantitative analysis, Spectrochim. Acta B 160 (2019) 105688, , https://doi.org/10.1016/j.sab.2019.105688.
[40] E. McIntee, E. Viglino, C. Rinke, S. Kumor, L. Ni, M.E. Sigman, Comparative analysis of automotive paints by laser induced breakdown spectroscopy and nonparametric permutation tests, Spectrochim. Acta B 65 (2010) 542–548, https://doi.org/10.1016/j.sab.2010.04.021.
[41] P. Lucena, I. Gaona, J. Moros, J.J. Laserna, Location and detection of explosive-contaminated human fingerprints on distant targets using standoff laser-induced breakdown spectroscopy, Spectrochim. Acta B 85 (2013) 71–77, https://doi.org/10.1016/j.sab.2013.04.003.
[42] M.M. El-Deftar, N. Speers, S. Eggins, S. Foster, J. Robertson, Ch. Lennard, Assessment and forensic application of laser-induced breakdown spectroscopy (LIBS) for the discrimination of Australian window glass, Forensic Sci. Int. 241 (2014) 46–54, https://doi.org/10.1016/j.forsciint.2014.04.040.
[43] B. Woods, K.P. Kirkbride, Ch. Lennard, J. Robertson, Soil examination for a forensic trace evidence laboratory – part 2: elemental analysis, Forensic Sci. Int. 245 (2014) 195–201, https://doi.org/10.1016/j.forsciint.2014.10.018.
[44] M. Tofanelli, L. Pardini, M. Borrini, F. Bartoli, A. Bacci, Al. D'Ulivo, E. Pitzalis, M.C. Mascherpa, S. Legnaioli, G. Lorenzetti, S. Pagnotta, G. de Holanda Cavalcanti, M. Lezzerini, V. Pallesch, Spectroscopic analysis of bones for forensic studies, Spectrochim. Acta B 99 (2014) 70–75, https://doi.org/10.1016/j.sab.2014.06.006.
[45] M.M. El-Deftar, J. Robertson, S. Foster, Ch. Lennard, Evaluation of elemental profiling methods, including laser-induced breakdown spectroscopy (LIBS), for the differentiation of Cannabis plant material grown in different nutrient solutions, Forensic Sci. Int. 251 (2015) 95–106, https://doi.org/10.1016/j.forsciint.2015.03.029.
[46] F.J. Fortes, M.D. Perez-Carceles, A. Sibon, A. Luna, J.J. Laserna, Spatial distribution analysis of strontium in human teeth by laser-induced breakdown spectroscopy: application to diagnosis of seawater drowning, Int. J. Legal Med. 129 (2015) 807–813, https://doi.org/10.1007/s00414-014-1131-9.
[47] D. Prochazka, M. Bilík, P. Prochazková, M. Brada, J. Klus, P. Pořízka, J. Novotný, K. Novotný, B. Ticová, A. Bradáč, M. Semela, J. Kaiser, Detection of visually unrecognizable braking tracks using laser-induced breakdown spectroscopy, a feasibility study, Spectrochim. Acta B 118 (2016) 90–97, https://doi.org/10.1016/j.sab.2016.02.013.
[48] M. López-López, C. Alvarez-Llamas, J. Pisonero, C. García-Ruiz, N. Bordel, An exploratory study of the potential of LIBS for visualizing gunshot residue patterns, Forensic Sci. Int. 273 (2017) 124–131, https://doi.org/10.1016/j.forsciint.2017.02.012.
[49] Ch. Lennard, M.M. El-Deftar, James Robertson, Forensic application of laser-induced breakdown spectroscopy for the discrimination of questioned documents, Forensic Sci. Int. 254 (2015) 68–79, https://doi.org/10.1016/j.forsciint.2015.07.003.
[50] N. Elsherbiny, O. Aied Nassef, Wavelength dependence of laser induced breakdown spectroscopy (LIBS) on questioned document investigation, Sci. Justice 55 (2015) 254–263, https://doi.org/10.1016/j.scijus.2015.02.002.
[51] M. Hoehse, A. Paul, I. Gornushkin, U. Panne, Multivariate classification of pigments and inks using combined Raman spectroscopy and LIBS, Anal. Bioanal. Chem. 402 (2012) 1443–1450, https://doi.org/10.1007/s00216-011-5287-6.
[52] T. Trejos, R. Corzo, K. Subedi, J. Almirall, Characterization of toners and inkjets by laser ablation spectrochemical methods and scanning electron microscopy-energy dispersive x-ray spectroscopy, Spectrochim. Acta B 92 (2014) 9–22, https://doi.org/10.1016/j.sab.2013.11.004Get rights and content.
[53] K. Subedi, T. Trejos, J. Almirall, Forensic analysis of printing inks using tandem

laser induced breakdown spectroscopy and laser ablation inductively coupled plasma mass spectrometry, Spectrochim. Acta B 103-104 (2015) 76–83, https://doi.org/10.1016/j.sab.2014.11.011.
[54] L. Holmes, D. Treacher, C. Michelbach, Tipler radiation shielding, J. Phys. Spec. Topics 13 (2014) 1–2 https://www108.lamp.le.ac.uk/ojs1/index.php/pst/article/view/2221/2125.
[55] J. H. Hubbell, S. M. Seltzer, Tables of X-ray Mass Attenuation Coefficients and Mass Energy-Absorption Coefficients (Version 1.4), National Institute of Standards and Technology, Gaithersburg, MD. http://physics.nist.gov/xaamdi, (accessed 13 Jan. 2020).
[56] L. Drake, How Deep Can You Measure? http://www.xrf.guru/Concepts/DepthOfAnalysis/index.html, (accessed 13 Jan. 2020).
[57] T. Lera, J. Giaccai, N. Little, A scientific analysis of the first issues of Chile 1853–1862, London printing, Smithsonian contributions to history and technology, in: T. Lera, J.H. Barwis, D.L. Herendeen (Eds.), Proceedings of the First International Symposium on Analytical Methods in Philately, Smithsonian Institution, Washington DC, 2013, pp. 19–33.
[58] https://www.nbp.pl/homen.aspx?f=//bezpiecznepieniadze/wszystkie_banknoty_en.html (accessed 13 Jan. 2020).
[59] L.D. Spence, A.T. Baker, J.P. Byrne, Characterization of document paper using elemental compositions determined by inductively coupled plasma mass spectrometry, J. Anal. At. Spectrom. 15 (2000) 813–819, https://doi.org/10.1039/B001411G.
[60] J. El Haddad, L. Canioni, B. Bousquet, Good practise in LIBS analysis: review and advices, Spectrochim. Acta B 101 (2014) 171–182, https://doi.org/10.1016/j.sab.2014.08.039.
[61] W. Hübert, G. Ankerhold, Elemental misinterpretation in automated analysis of LIBS spectra, Anal. Bioanal. Chem. 400 (2011) 3273–3278, https://doi.org/10.1007/s00216-011-4793-x.